# Homology Model-Based Virtual Screening for GPCR Ligands Using Docking and Target-Biased Scoring

Sebastian Radestock,[†] Tanja Weil, and Steffen Renner*[,‡]

Chemical R&D, Merz Pharmaceuticals GmbH, Eckenheimer Landstrasse 100, D-60318 Frankfurt am Main, Germany

Received January 21, 2008

The current study investigates the combination of two recently reported techniques for the improvement of homology model-based virtual screening for G-protein coupled receptor (GPCR) ligands. First, ligand-supported homology modeling was used to generate receptor models that were in agreement with mutagenesis data and structure−activity relationship information of the ligands. Second, interaction patterns from known ligands to the receptor were applied for scoring and rank ordering compounds from a virtual library using ligand−receptor interaction fingerprint-based similarity (IFS). Our approach was evaluated in retrospective virtual screening experiments for antagonists of the metabotropic glutamate receptor (mGluR) subtype 5. The results of our approach were compared to the results obtained by conventional scoring functions (DockScore, PMF-Score, Gold-Score, ChemScore, and FlexX-Score). The IFS lead to significantly higher enrichment rates, relative to the competing scoring functions. Though using a target-biased scoring approach, the results were not biased toward the chemical classes of the reference structures. Our results indicate that the presented approach has the potential to serve as a general setup for successful structure-based GPCR virtual screening.

## INTRODUCTION

G-protein coupled receptors (GPCRs) are among the most important drug targets for the pharmaceutical industry.[1] More than 30% of all marketed therapeutics interact with them.[1] However, these drugs only target about 30 members of this family and in most cases Class A GPCRs (biogenic amine receptors).[2] There is a promising therapeutic potential to exploit the remaining family members.[3] In this context, Class C GPCRs and in particular metabotropic glutamate receptors (mGluRs) have attracted interest due to their role as modulators of glutamatergic and other major neurotransmitter systems in the central nervous system (CNS).[4,5]

Since GPCRs are integral membrane proteins, an experimental determination of their tertiary structure is highly challenging. Usually, detailed structural information is inferred by homology from the structure of bovine rhodopsin, which until recently was the only GPCR for which a crystal structure was resolved,[6,7] or by using de novo structure prediction strategies.[8–11] Recently, the crystal structure of an engineered $\beta_2$ adrenergic GPCR has been determined.[12] Both structures represent Class A GPCRs, and therefore it is not yet clear how well they can be applied as templates for accurate models of other GPCR classes. As a consequence of the lack of crystal structures, computational design of modulators for GPCRs is most often accomplished via structure-based approaches grounded on homology models or by using ligand-based virtual screening methods.

Ligand-based in silico approaches have been shown to be particularly valuable for the identification of initial hits. These methods are often based on the concept of molecular similarity, that states that molecules with similar features likely exhibit similar biological responses.[13] By applying ligand-based virtual screening methods, successful computer-aided drug discovery for GPCRs, including mGluRs, has been achieved.[14–17] Ligand-based approaches generally bear the advantage that they are fast and therefore allow virtual screening of large databases of hundreds of thousands of compounds. Though many ligand-based methods allow for the retrieval of novel or alternative molecular scaffolds,[18–21] the optimization of the initial hits is often considered challenging since ligand-based methods generally lack any information on how the potential ligands might bind to the receptor binding site.

Structure-based methods are particularly helpful to understand how a potential ligand might bind to the receptor.[22] These approaches were traditionally employed for lead optimization purposes but are progressively used for hit identification processes, too.[23,24] Of central importance to the structure-based in silico approaches is the ability to generate and identify relevant binding modes and to accurately rank order small molecules according to their affinity to the target by applying docking techniques.[25] Assuming that near native receptor−ligand configurations are produced, the general advantage of molecular docking is that the visual analysis of interactions between the binding partners allows for an intuitive interpretation and understanding of the binding process at the receptor binding site. In recent years, homology models of GPCRs based upon the template

* Corresponding author phone: +49-231-133-2432; e-mail: steffen.renner@mpi-dortmund.mpg.de.

[†] Current address: Fachbereich Biowissenschaften, Molekulare Bioinformatik, Johann Wolfgang Goethe-Universität, Max-von-Laue-Strasse 9, D-60438 Frankfurt am Main, Germany.

[‡] Current address: Department IV - Chemical Biology, Max-Planck-Institut für Molekulare Physiologie, Otto-Hahn-Strasse 11, D-44227 Dortmund, Germany.

10.1021/ci8000265 CCC: $40.75 
Published on Web 04/26/2008

structure of bovine rhodopsin have been successfully utilized for structure-based virtual screening.[9,26–33]

The general performance of structure- and ligand-based approaches for virtual screening of GPCRs has recently been compared.[33] The evaluation of different methods in retrieving known antagonists from virtual libraries showed that ligand-based virtual screening techniques generally outperform the molecular docking approach when sufficient ligand information is used for the generation of the models. However, it was concluded that the docking approach is most helpful for understanding how ligands of different chemotypes potentially bind to the receptor. For using homology model-based approaches in virtual screening the problem is often related to the fact that the models are not accurate enough to be used for molecular docking[34] and that the functions used for scoring and rank ordering the potential ligands are not performing well on homology models or low resolution structures.[35]

To improve the accuracy of the models, the homology modeling process is frequently supported by other techniques such as 3D QSAR or site directed mutagenesis. For instance, Bissantz et al. demonstrated that their homology models of the dopamine D3, muscarinic M1, and vasopressin V1a receptors were reliable enough to retrieve known antagonists in a retrospective virtual screening experiment.[28] A knowledge- and pharmacophore-based procedure was used to develop models of the agonists activated receptors.

An alternative approach (MOBILE) was developed by Evers et al., combining homology modeling and 3D QSAR.[36] Here, a pharmacophore-based alignment of active ligands is used as an "environment" during model calculation, and it has been shown that this procedure results in more relevant geometries of the receptor binding sites. MOBILE has been applied successfully to model the structure of the neurokinin-1 (NK1) receptor. Using this receptor in a virtual screening experiment, a ligand with binding affinity in the submicromolar range was identified.[26] Similarly, this method has been applied to the $\alpha_{1A}$ adrenergic receptor.[32]

The principles of molecular similarity and molecular recognition have been combined in "target-biased" schemes in order to improve the general accuracy of the scoring functions used in structure-based design applications.[37–39] In the field of docking, similarity-driven approaches have been introduced that take advantage of additional structural information about ligands already known to bind to the target as well as protein-based information, such as receptor-based pharmacophores or "hot-spot" analyses of binding sites.[40–44] By inferring ligand-based information from sequence analysis, site directed mutagenesis, and other functional studies, these approaches can also be applied to homology models, i.e., where no detailed information about the tertiary structure of receptor−ligand complexes is available.

Using a hybrid pharmacophore- and homology model-based database searching approach, Varady et al. reported the discovery of novel potent dopamine D3 receptor ligands.[30,31] Similarly, Evers et al. used FlexX-Pharm[40] for docking a database of compounds against the modeled binding site of the NK1 receptor.[26] Here, a structure-based pharmacophore hypothesis has been generated considering mutational data from literature and the features common to all known NK1 antagonists.

In the present study, the combination of the two above-mentioned techniques for the improvement of homology model-based virtual screening was investigated. First, ligand-supported homology modeling was applied.[36] Clues to infer the binding modes of the ligands were provided by data from site directed mutagenesis. Second, to rank order docking solutions, a target-based scoring scheme was developed exploiting the patterns of interactions between ligands already known to bind to the target and the binding site. As reference ligands, the compounds that have already been employed in ligand-supported homology modeling were used. Patterns of interactions were encoded in binary ligand−receptor fingerprints.[45]

Using fingerprints to incorporate ligand-based information into a structure-based approach has been introduced by Deng et al. (with a particular focus on protein kinases) as the SIFt structural interaction fingerprint approach. It has been shown in either residue-based[46] or atom-based implementations[47,48] to outperform conventional scoring schemes in predicting correct poses for druglike compounds. In the present study, a very simple interaction fingerprint representation was used to account for the intrinsic inaccuracy of a homology model.

Our scoring methodology, subsequently referred to as the interaction fingerprint-based similarity (IFS), has been tested in retrospective virtual screening experiments against mGluR subtype 5. It is expected that the identification of negative allosteric modulators (NAMs) for mGluR5 will open up therapeutic possibilities to treat pain, anxiety, or Parkinson's disease.[4,49] To put the results into proper perspective, docking solutions were also rank ordered using five conventional scoring functions (Dock-Score, PMF-Score, Gold-Score, ChemScore, and FlexX-Score). We show that our mGluR5 homology model was reliable enough to discriminate between known antagonists and inactive druglike molecules.

## METHODS

The general strategy for homology model-based virtual screening using the target-based scoring scheme pursued in the present study is presented in Figure 1. In the first step, a model of mGluR5 was generated by applying reference ligand-supported homology modeling. Side chains were manually optimized until the assumed binding modes of the reference ligands could be reproduced by docking simulations. Then, a database of druglike molecules was docked against the receptor, following a simple virtual screening protocol with FlexX.[50] In this step, only structural information about the protein environment was taken into account. Information about the patterns of interactions between the reference compounds and the binding site residues was used to rank order the docking solutions (third step). Here, predicted patterns of interactions of the docking solutions were compared with the patterns of interactions of the reference ligands. Conceptually, patterns of interactions were encoded in binary fingerprints.[45] The similarity between two fingerprints was determined via the Tanimoto coefficient.[51] Our scoring methodology is referred to as the interaction fingerprint based similarity (IFS).

**Ligand-Supported Homology Modeling of mGluR5.** For ligand-supported homology modeling, the first step included the selection of a set of ligands and to constrain homology models to enable a set of predefined interactions to be

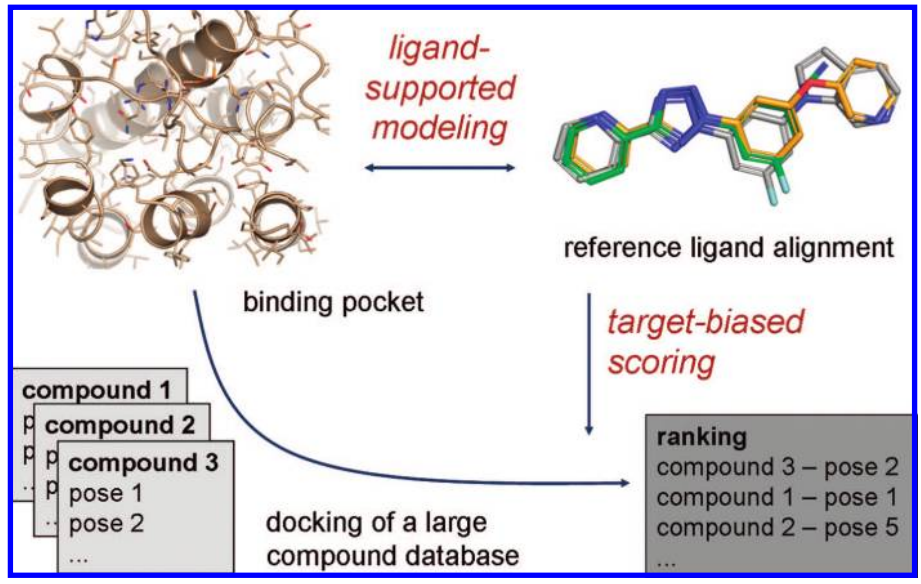


**Figure 1.** Generation of a protein-specifically adapted scoring scheme.

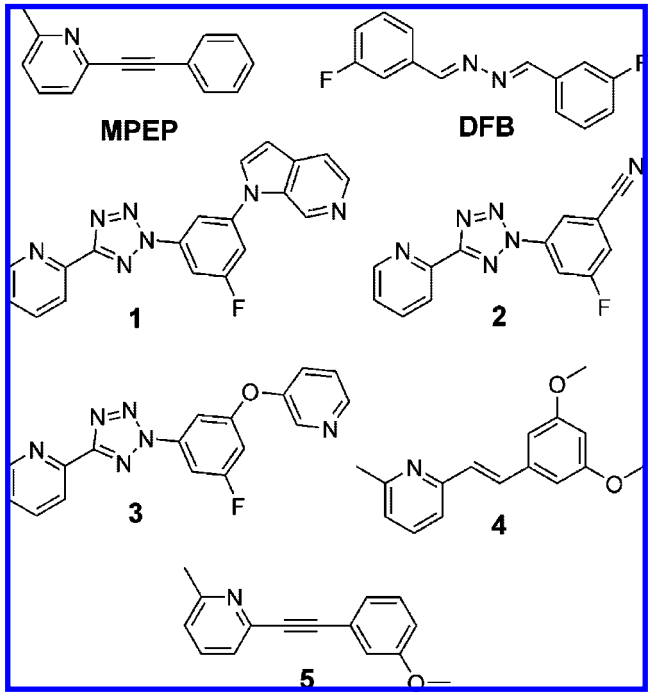


**Figure 2.** Allosteric ligands of mGluR5.

formed.[26,32] For mGluR5, the only published data of mutations affecting ligand binding covered three small and structurally similar negative allosteric modulators (NAMs) 2-methyl-6-(phenylethynyl)pyridine (MPEP) (Figure 2),[52] M-MPEP,[53] and Fenobam[54] and one positive allosteric modulator (PAM), DFB (Figure 2).[55] Unfortunately, the information gained with these ligands did not allow for unambiguous conclusions regarding the binding mode of larger mGluR5 NAMs with different patterns of potential interactions. Thus, unlike the well studied biogenic amines that were used in the studies by Evers et al.,[26,32] a binding mode for larger, non-MPEP-like mGluR5 NAMs had to be established before performing homology modeling and virtual screening.

Since the mutational data for mGluR5 NAMs alone were not sufficient to predict a binding mode, an alternative approach integrating ligand binding mode information from the entire family of GPCRs was selected, which was motivated by two recently published chemogenomics approaches for the GPCR family.[56,57] In these two studies, the GPCR protein family was clustered based on the residues from a general ligand binding site that was defined around the binding site of retinal in bovine rhodopsin. Focusing on residue positions that were identified within these studies, one likely binding mode was found that was compatible with the observed SAR and mutational data.

The mGluR5 homology model was calculated according to an adapted version of a ligand-supported homology modeling approach (MOBILE) developed by Evers et al.,[36] using a pharmacophore-based alignment of active ligands as an "environment" during homology model calculation. Side chain conformations were further refined until ligand binding modes could be reproduced by molecular docking.

In order to derive a ligand alignment and a binding mode hypothesis of mGluR5 NAMs, a set of ligands was chosen which combined the availability of SAR information and a higher molecular complexity compared with MPEP that has only the pyridine nitrogen as single potential electrostatic interaction partner. Three molecules, tetrazole pyridines **1**, **2**, and **3** (Figure 2),[58] were selected from a recently published series of NAMs (all with a system of at least three nonfused aromatic rings with a central tetrazole) for which a large number of SAR data has been published.[58–62] The selected molecules could be considered as potent end points of the activity optimization process, with functional human mGluR5 $IC_{50}$ values of 3.9, 6.7, and 16 nM, for compounds **1**, **2**, and **3**, respectively. The tetrazole pyridines were designed as mimics of MPEP, and the tetrazole moiety was assumed to replace the ethynyl linker of MPEP.

Two other molecules were selected on the basis that they might interact with the receptor in a similar fashion compared to the tetrazole pyridines: MRZ 2084 (**4**) and M-MPEP[53] (**5**) both represent potent mGluR5 NAMs (Figure 2). MRZ 2084 bears two additional favorable methoxy groups compared to one of the first reported mGluR5 NAMs in literature, SIB-1893,[63] and M-MPEP has one additional favorable methoxy group compared to MPEP, leading to increased functional activities.

Ligand alignments were calculated with the flexible alignment tool in MOE,[64] using the "Refine Existing Alignment" option. The mGluR5 homology model was calculated on the basis of an existing homology model for the transmembrane domain of mGluR1,[65,66] a receptor with a high structural homology with respect to mGluR5. This model was successfully used to explain SAR data of mGluR1.[65,66] The derivation of the mGluR1 homology model is described in the Supporting Information.

Homology models were calculated using an approach based on a ligand-supported homology modeling method (MOBILE) developed by Evers et al.[36] Sets of receptor models were calculated using MOE.[64] Since the initial (unbound) receptor models did not allow for good docking results (mainly because side chains pointed into the binding site and prevented the ligands from entering the binding site), a modified version of the strategy was applied. The hypothesis of the ligand overlay was used directly in the homology model calculation using the "Environment" option in MOE which forces the algorithm to consider interaction energies with the environment. This model was then evaluated by docking the reference ligands back into the binding site using FlexX 1.2,[50] as implemented in the 7.2 release of the Sybyl package,[67] with standard settings. Side chains were manually optimized until the desired binding modes were reproduced successfully. The final conformations of the ligands were used as references for the interaction fingerprint scoring. To name residues in the text for discussion, the residue numbering scheme proposed by Ballesteros and Weinstein[68] was applied.

**Data Sets for Virtual Screening.** The performance of the target-biased scoring scheme was evaluated in retrospective virtual screening experiments. The experiments were carried out ten times, using ten different screening sets, each consisting of a small number of different known actives and a large number of inactive compounds.

A total of 159 mGluR5 NAM structures and their affinities were taken from the literature and from recent patent information,[58–62 69–81] and duplicates were removed. Affinities of the compounds were also collected, given as $IC_{50}$ values, and ranged from low micromolar to low nanomolar (4.9 $\mu$M to 3.02 nM). The known actives belonged to six structurally distinct scaffold classes: 61 compounds derived from MPEP or the structurally related mGluR5 NAM MTEP (3-[(2-methyl-4-thiazolyl)ethynyl]pyridine), 52 tetrazole pyridines, 14 dipyridyl amides, 12 thiopyrimidines, 15 phenyl ureas, and 5 benzoxazoles (Table S1 in the Supporting Information). The size of each group varied significantly. A visual inspection revealed that the diversity within each group was limited due to the fact that several compounds belonged to the same structural series. To minimize the chance of any potential bias toward a certain structural class during virtual screening, ten subsets (of 30 compounds each) were randomly selected. Each subset was composed of six MPEP/MTEP derivatives, six tetrazole pyridines, three benzoxazoles, and five molecules from each of the remaining scaffold groups.

Presumably inactive compounds were taken from the National Cancer Institute (NCI) Diversity Set chemical library (http://dtp.nci.nhi.gov/dscb/diversity_explanation.html). This data set represents a diverse set of druglike compounds, and it has already been used successfully in other structure-based virtual screening studies.[82] Noteworthy, these molecules were only assumed to be inactive with no experimental evidence that there is no cross reactivity with mGluR5.

For 228 compounds of the inactive set, the docking algorithm (FlexX) failed to calculate a solution, i.e., due to difficulties in base fragment placement or incremental growing during the docking process. These compounds were discarded from the inactive set, resulting in a total number of 1792 inactive compounds. The whole set of inactive compounds was mixed with each of the ten subsets of known active compounds, thus resulting in ten different data sets for virtual screening. Each screening set contained 1822 compounds in total. The ratio of active to inactive compounds was 1:60 which is in the range of ratios chosen in similar studies, e.g., a ratio of 1:99 was chosen by Bissantz et al.,[28] and a ratio of 1:19 was chosen by Evers et al.[33]

Before running the virtual screening experiments, molecular properties were calculated for the compounds in the screening sets. Following a suggestion by Seifert,[83] the molecular weight in Da (MW), the ratio of rotatable bonds to the total number of bonds (b_rotR), the positively charged fractional solvent accessible surface area (FASA+), and the polar fractional solvent accessible surface area (FASA_P) were chosen as descriptors. The associated properties are not correlated to each other, as shown for the World Drug Index (WDI) chemical library, where $R^2 < 0.07$.[83] The descriptors were calculated using MOE,[64] using all 159 known active compounds.

Property distributions for the inactive compounds were compared to the corresponding property distributions for the known actives. This was primarily done to ensure that no obvious systematic differences in structures and properties occurred between the known actives and the inactives and to minimize the chances of introducing any potential bias in favor of the former. The results are shown in Figure 3: In all property distributions over the ranges indicated, there were no clear differences between known actives and inactive compounds. This observation has further been quantified using analysis of variance (ANOVA). ANOVA was performed as described in the Supporting Information. The $\eta^2$ coefficient from ANOVA measures the power of a physicochemical property to discriminate between active and inactive compounds. ANOVA results were obtained using *all* 159 active and 1792 inactive compounds. The discriminatory power of the physiochemical properties was significant but very low (MW: $\eta^2 = 0.5\%$, $F = 11.72$; b_rotR: $\eta^2 = 0.7\%$, $F = 15.18$; FASA+: $\eta^2 = 1.9\%$, $F = 43.41$; FASA_P: $\eta^2 = 3.9\%$, $F = 87.8$); therefore, the sets of active compounds were considered sufficiently alike to provide a rigorous test of the discriminatory capability of different scoring schemes.

**Interaction Fingerprints.** The scoring scheme presented in this study is based on the incorporation of receptor−ligand interaction information from reference ligands already known to bind to the receptor. As reference ligands, all compounds that have already been employed to support homology modeling were used. Patterns of interactions were modeled using binary ligand−receptor fingerprints.

To generate the interaction fingerprints, each of the reference ligands was docked into the receptor binding site using FlexX 1.2,[50] as implemented in the 7.2 release of the

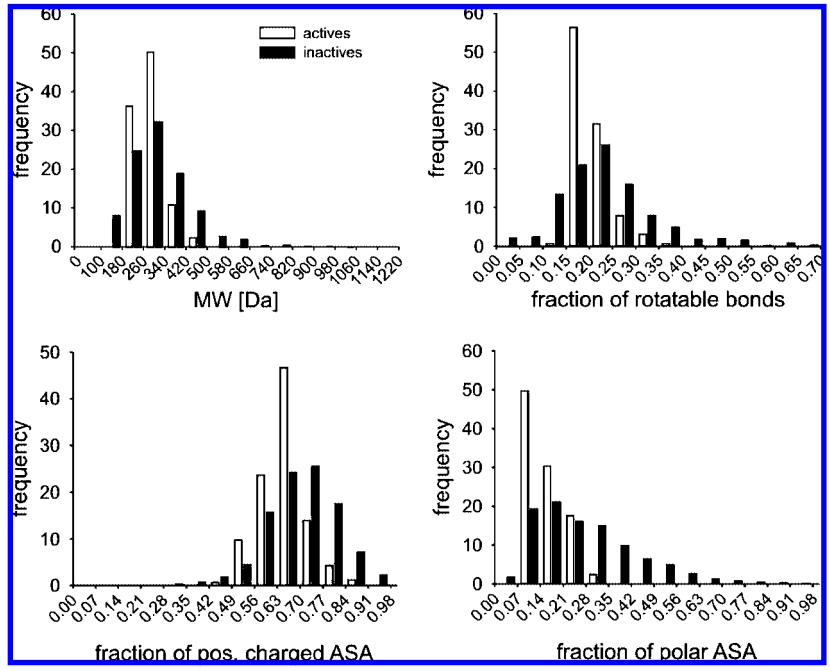


**Figure 3.** Physicochemical profile of the mGluR5 specific known active and inactive set of compounds. Property distributions of the actives were calculated using all 159 known active compounds.

Sybyl package.[67] The best solution was determined visually, considering mutational data and the features common to all considered reference ligands. In FlexX, an interaction geometry database was used to exactly describe intermolecular interaction patterns.[50] FlexX recognizes the interactions between the reference ligand and the receptor. All information about the type and the strength of each interaction, and about the amino acid of the receptor involved, was written to a file. This file was used to generate the interaction fingerprint, where a single bit was used to account for an interaction between a ligand and a particular residue.

In total, 53 binding site residues were defined. The residues are listed in the Supporting Information. All information about the type and the strength of the interaction was discarded. In addition, the incorporation of more sophisticated information, including binding energies or distinguishing between different interactions like hydrogen bonds or hydrophobic interactions, did not improve the results (data not shown). Furthermore, the simpler the fingerprint is, the faster the calculations are.

**Virtual Screening, Docking, And Scoring.** Docking of the compounds in the test sets was performed using FlexX 1.2,[50] as implemented in the 7.2 release of the Sybyl package.[67] Active site atoms were defined by choosing the atoms that were located in spheres of 8 Å radius around the atoms of the reference ligands by applying a residue-based cutoff. The consistency of polar hydrogen positions of the receptor was checked manually. Standard parameters were used for base fragment placement, iterative growing and subsequent scoring of the poses. Atom and bond types were automatically assigned to the compounds. Starting geometries of the compounds were randomized. Partial charges and protonation states were assigned on a template basis. For each compound, the top 30 solutions were retained and scored using the IFS-based scoring scheme and using five conventional scoring functions for comparison.

The scoring process consisted of two steps: (1) the selection of the best pose from the 30 docking solutions for each test compound and (2) the ranking of all best poses. For every virtual screening experiment, in both steps the same scoring scheme was used. The combination of different scoring schemes only gave results that were strongly determined by the weakest scheme (results not shown).

In our target-biased scoring scheme, the "score" was defined as the maximal similarity between the pattern of ligand−receptor interactions of a docking solution and the interaction pattern of one of the reference ligands. The similarity was quantified by comparing the interaction fingerprint of each docking pose with the fingerprints of the reference ligands and by calculating the Tanimoto coefficient[51] that ranges between 0 and 1, where 1 indicates the identity of two fingerprints.

As conventional scoring schemes, we used the functions implemented in the Sybyl CScore module (Dock-Score, PMF-Score, Gold-Score, ChemScore) and the function implemented as objective function in the docking algorithm FlexX (FlexX-Score). In all cases, default settings were used.

Docking solutions were also rank ordered using two simple guided docking scoring functions that incorporated two different pharmacophoric constraints. This aimed at filtering docking solutions that were placed outside the binding pocket by the docking engine (FlexX). For every docking solution it was checked whether the pharmacophoric constraint was satisfied. If this was the case, the pose was scored using FlexX-Score. Otherwise, the pose was assigned a score of 0. As pharmacophoric constraints we used the interaction with R647 and the interaction with W784. These constraints were assumed to be well suited as indicators for a compound placed within the binding site because they were satisfied by most docking poses that were placed within the binding site.

**Analysis of the Virtual Screening Results.** The effectiveness of the scoring scheme was evaluated by assessing the enrichment of known active compounds within the top-ranked compounds compared to randomly selected ones. The enrichment factor was calculated as described in the Sup-

porting Information. Halgren et al. pointed out that enrichment factors at the top-scored *x*% of the ranked database take no account of the ranks of the known actives.[84] It has been proposed that quoting enrichment factors at several values of *x*, or showing the enrichment curve plot, is advisable. Thus, in our case, for each of the six scoring schemes applied, enrichment factors at the top-scored 1, 5, and 10% of the ranked database are reported. We performed ten virtual screening experiments with different sets of known actives. Hence, our results are given by reporting the mean enrichment factor and the standard deviation. Enrichment curves were calculated from the average values of the ten experiments at each top position of the database. For the enrichment curves, standard deviations were not shown for sake of clarity. Instead, we report the standard deviations only for the enrichment factors at the top-scored 1, 5, and 10% of the ranked database.

To further quantify the performance of a scoring scheme in virtual screening, analysis of variance (ANOVA) was used to measure the discriminatory power of the scoring scheme. ANOVA was performed as described in the Supporting Information. It has been suggested that ANOVA is a useful measure to assess the power of a scoring function.[83] The $\eta^2$ coefficient from ANOVA measures the power of a scoring function to discriminate between active and inactive compounds. Further, it has been demonstrated by in silico experiments that $\eta^2$ is less artifact-prone and therefore more suitable for algorithm development compared to enrichment factors, which in turn are more diagnostic for the practical performance of virtual screening.[83]

ANOVA results were obtained using *all* 159 active and 1792 inactive compounds. In the case of the target-biased scoring scheme, compounds that were assigned an IFS of 0 were discarded. This action was motivated by the notion that an IFS of 0 indicates that these compounds have not been accommodated within the binding site by the docking algorithm. This it is *not* due to weaknesses in the scoring scheme but due to deficiencies of the docking algorithm and/or due to inaccuracies in the receptor binding site geometry. A good scoring function should recognize these compounds that have not been docked into the binding site and assign them a low score, regardless their true activity. We also tried to perform ANOVA using the whole distribution of the IFS (results not shown).

## RESULTS AND DISCUSSION

**Generation of an Antagonist-Bound Homology Model of mGluR5.** The first step in the calculation of a ligand-supported homology model was to select a set of appropriate reference ligands. The five selected reference ligands **1**−**5** are shown in Figure 2. All three NAMs for which binding data was reported from mutated mGluR5 (MPEP, [52] M-MPEP,[53] and Fenobam[54]) were relatively small molecules consisting only of two rings connected via a linker. For MPEP, Malherbe et al. suggested a binding mode, where the pyridine nitrogen interacts with T780 (6.44) via a hydrogen-bond, and $\pi$-$\pi$ interactions were proposed between MPEP and Y658 (3.40). The MPEP binding site was restricted on both ends parallel to the axis of the retinal pocket via L743 (5.47) in TM5 and by W784 (6.48) and P654 (3.38) on the other side. In our model, larger ligands did not fit into this small pocket. In the MPEP and Fenobam mutational studies, the authors also identified residues Y791 (6.55) and R647 (3.29) having an effect on the activity of the ligands. Both residues seemed to be located too far apart from the proposed binding site to interact directly with the ligands and were thus proposed to have an indirect effect.[52,54] The two residues are located directly in the retinal site, and mutations at these positions have been reported to affect ligand binding for other GPCRs (e.g., on the melanocortin-1 receptor[85] or the gonadotropin-releasing hormone receptor[86] for 3.29 and the A3 adenosine receptor[87] for 6.55). This indicates that the proposed binding mode of Malherbe et al. for MPEP might not be suited to explain all observed mutational data reported, which could suggest that another binding mode might exist for mGluR5 NAMs. Based on these observations, the mGlu5 receptor was explored for alternative binding modes for the larger mGluR5 ligands.

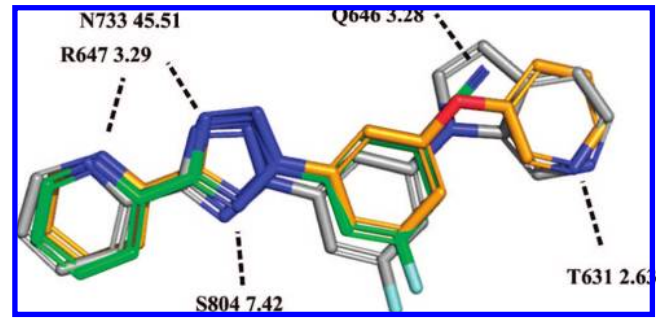


**Figure 4.** Proposed binding mode of the tetrazole mGluR5 NAMs that was used for receptor modeling and as a reference for the virtual screening.

It is well-known for Class A GPCRs that these receptors share a common binding site located at the corresponding residues around the retinal binding site in bovine rhodopsin.[56,57] Clustering all GPCRs on the basis of the residues of this general binding pocket was shown to lead to similar results compared to full sequence-based clustering.[56,57] Analysis of publicly available mutational data on Class C GPCRs from mGluR5,[53–55,88] mGluR1,[52,89] the extracellular calcium-sensing receptor (CaSR),[90–92] and the sweet taste receptor subunit T1R3[93,94] gave that many of the important residue positions were overlapping with the proposed general binding site from Class A GPCRs, indicating that a comparable general binding site might be present in Class C GPCRs.

As a starting point for the identification of the binding mode of the tetrazole pyridine ligands **1**, **2**, and **3** (Figure 2), all possible low energy alignments were generated and ranked by their potential hydrogen-bonding interaction pattern with polar residues of the general binding pocket in mGluR5. A schematic representation of the best identified binding mode is given in Figure 4. Molecular docking was applied in order to evaluate the proposed binding mode. For the more MPEP-like ligands **4** and **5** (Figure 2) binding modes were selected that best overlapped with the selected binding mode of the tetrazole pyridines. The alignment of the five ligands was used as environment in the homology modeling procedure. The best poses generated by the docking algorithm for each of the ligands were also used as references in the virtual screening procedure.

The diversity of the generated binding modes was assessed in terms of their potential patterns of interactions with the receptor binding site. The information on the patterns of

interactions of the compounds was encoded in binary strings (interaction fingerprints). The similarity between two fingerprints was calculated using the Tanimoto coefficient. In the following, this similarity measure is referred to as the interaction fingerprint-based similarity (IFS). The average IFS between poses of reference ligands was 0.47 ± 0.16. The highest mutual similarity was found between the two MPEP-like ligands **4** and **5** (Figure 2) with an IFS of 0.9. The least similar were the tetrazole pyridine ligands **1** and **3** (Figure 2) with an IFS of 0.3. Apparently, for the set of ligands used in this study, the size of the ligands had a larger effect on binding mode diversity than the underlying chemical structure, due to the fact that different numbers of interactions could be formed. Using more diverse ligands of the same size might therefore not contribute to the scoring function unless additional interaction points are addressed or different combinations of interactions are realized.

**Virtual Screening for Antagonists of mGluR5.** The general strategy for virtual screening is illustrated in Figure 1. It is important to note that only information on *patterns of ligand−receptor interactions* was incorporated and no *structural features of the ligands* were recognized. As reference ligands the compounds that have previously been employed for ligand-supported homology modeling were used. As described above, the putative binding mode of these ligands could be inferred from mutagenesis data. The information on the patterns of interactions of the compounds was encoded in binary strings (interaction fingerprints). Interaction fingerprints were generated for the reference compounds and for all docking poses of the screening set compounds during the virtual screening experiment. As a "score", the maximal similarity between the fingerprint of each docking pose and one of the reference fingerprints was calculated using the Tanimoto coefficient. Here, the interaction fingerprint-based similarity (IFS) is directly used as a "score".

First, a summary analysis that compares the general performance of the IFS-based scoring scheme with the general performance of five conventional (i.e., purely structure-based) scoring functions (PMF-Score, FlexX-Score, ChemScore, Dock-Score, and Gold-Score) is discussed. In retrospective virtual screening, the selection of compounds in the data set (screening set) is one of the most important steps that influence the outcome of the experiment and the general validity of the results. In this context, it has been suggested that one should use a homogeneous data set, where the inactive compounds have similar properties to the known active compounds.[83,95] In the present study, 159 known negative allosteric mGluR5 modulators (NAMs) with functional $IC_{50}$ values below 4.9 $\mu$M were used as "active" compounds, compiled from patents and literature. The active compounds belonged to six different scaffold classes (see below). 1792 presumably inactive compounds were taken from the NCI diversity set.

As shown in Figure 3, characteristic (pairwise uncorrelated) physicochemical properties of the active compounds are similar to the properties of the inactive compounds. Thus, we believe that virtual screening results are not biased due to the well-known tendency of a scoring function to favor larger molecules[96] or due to a potential tendency to favor or penalize more flexible, more polar, or highly charged molecules.

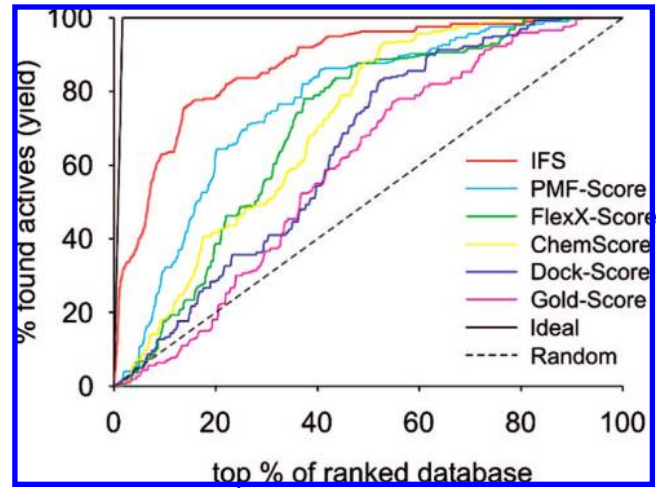


**Figure 5.** Enrichment curves obtained by docking the screening set compounds into the mGluR5 homology model using FlexX. Selection of the best docking pose and rank ordering of the docking solutions was performed using the target-biased scoring scheme and five conventional scoring functions.

Further analyses revealed that the active compounds were not distributed equally among six different scaffold classes. Thus, taking all actives may introduce bias and mislead interpretation of the results. Consequently, we decided to generate ten screening sets, each consisting of 30 known actives, where compounds are chosen randomly in such a way that in each set were six MPEP or MTEP derivatives, six tetrazole pyridines, five dipyridyl amides, five thiopyrimidines, five phenyl ureas, and three benzoxazoles. Each subset of known actives was mixed with the whole number of inactive compounds. This resulted in ten screening sets, each consisting of 1822 compounds. We are confident that these screening sets are suited for a valid analysis of our method and for a comparative analysis with other scoring functions.

In the first step, all screening compounds were docked against the receptor binding site using FlexX. Thereby, a large number of diverse docking solutions was generated for each compound. The docking poses were then rescored using the IFS-based scoring scheme and the five conventional scoring functions. For each compound, the pose yielding the highest score was selected, and the best poses for all compounds were rank ordered. Here, for both the selection and the rank ordering step the same scoring function was used. We also tried to use combinations of scoring functions, but the results were strongly determined by the weaker scoring function (results not shown).

Figure 5 shows the enrichment curves, computed as average over the ten virtual screening experiments. Standard deviations of the enrichment curves are given for the enrichment factors at the top-scored 1, 5, and 10% of the ranked database in Tables 1, 2, and 3. The curves show the enrichment of known active compounds within the top-ranked compounds compared to that of those randomly selected. Using the conventional scoring functions, the enrichment of active compounds among the top ranked molecules was poor. However, within the top scoring 10% of the molecules, most of the scoring functions performed better than a random selection. This indicates that our homology model was reliable enough to discriminate be-

**Table 1.** Enrichment Factors for the Top-Scored 10% of the Ranked Database

| | scoring scheme | | | | | |
|---|---|---|---|---|---|---|
| | IFS | PMF-Score | FlexX-Score | ChemScore | Dock-Score | Gold-Score |
| set 1 | 6.34 | 3.34 | 2.00 | 2.34 | 1.33 | 0.67 |
| set 2 | 6.67 | 3.34 | 2.00 | 2.00 | 1.67 | 0.67 |
| set 3 | 5.01 | 3.34 | 1.33 | 1.67 | 1.33 | 1.33 |
| set 4 | 6.67 | 2.67 | 1.67 | 2.00 | 1.33 | 0.00 |
| set 5 | 6.67 | 2.67 | 1.33 | 1.67 | 1.33 | 1.00 |
| set 6 | 6.67 | 3.00 | 2.00 | 2.00 | 1.33 | 0.67 |
| set 7 | 5.67 | 3.00 | 2.34 | 1.33 | 1.00 | 0.67 |
| set 8 | 6.01 | 4.00 | 1.67 | 1.33 | 2.00 | 1.00 |
| set 9 | 7.01 | 3.00 | 1.67 | 2.34 | 1.00 | 0.00 |
| set 10 | 6.34 | 3.34 | 1.67 | 1.33 | 0.67 | 0.33 |
| average[a] | 6.31 (0.60) | 3.17 (0.39) | 1.77 (0.32) | 1.80 (0.39) | 1.30 (0.37) | 0.63 (0.43) |
| optimal | 10.01 | 10.01 | 10.01 | 10.01 | 10.01 | 10.01 |
| random | 1.00 | 1.00 | 1.00 | 1.00 | 1.00 | 1.00 |

[a] The standard deviation is given in parentheses.

**Table 2.** Enrichment Factors for the Top-Scored 5% of the Ranked Database

| | scoring scheme | | | | | |
|---|---|---|---|---|---|---|
| | IFS | PMF-Score | FlexX-Score | ChemScore | Dock-Score | Gold-Score |
| set 1 | 9.96 | 2.65 | 1.33 | 1.99 | 0.00 | 0.66 |
| set 2 | 8.63 | 2.65 | 1.99 | 1.33 | 1.99 | 0.00 |
| set 3 | 5.31 | 1.99 | 1.99 | 1.99 | 1.33 | 1.33 |
| set 4 | 9.29 | 1.33 | 0.66 | 1.33 | 1.99 | 0.00 |
| set 5 | 7.96 | 1.99 | 1.99 | 1.99 | 1.33 | 0.66 |
| set 6 | 9.29 | 1.99 | 1.99 | 1.33 | 0.00 | 0.00 |
| set 7 | 6.64 | 1.33 | 0.66 | 1.33 | 0.00 | 0.66 |
| set 8 | 5.97 | 2.65 | 0.66 | 1.33 | 1.99 | 1.33 |
| set 9 | 9.29 | 2.65 | 1.33 | 1.33 | 1.33 | 0.00 |
| set 10 | 7.96 | 1.99 | 0.66 | 0.66 | 0.00 | 0.66 |
| average[a] | 8.03 (1.58) | 2.12 (0.52) | 1.33 (0.63) | 1.46 (0.42) | 1.00 (0.90) | 0.53 (0.52) |
| optimal | 20.02 | 20.02 | 20.02 | 20.02 | 20.02 | 20.02 |
| random | 1.00 | 1.00 | 1.00 | 1.00 | 1.00 | 1.00 |

[a] The standard deviation is given in parentheses.

**Table 3.** Enrichment Factors for the Top-Scored 1% of the Ranked Database

| | Scoring scheme |
|---|---|
| | IFS |
| set 1 | 26.55 |
| set 2 | 26.55 |
| set 3 | 13.27 |
| set 4 | 29.87 |
| set 5 | 26.55 |
| set 6 | 29.87 |
| set 7 | 19.91 |
| set 8 | 16.59 |
| set 9 | 19.91 |
| set 10 | 26.55 |
| average[a] | 23.56 (5.74) |
| optimal | 60.73 |
| random | 10.13 |

[a] The standard deviation is given in parentheses.

tween known antagonists and inactive druglike molecules and principally seems to be suitable for docking calculations.

The enrichment factors of the top-scored 10% of the ranked database are shown in Table 1. The PMF-Score function produced the best results out of the conventional scoring functions with an enrichment factor of $3.17 \pm 0.39$, reported as an average over the ten individual virtual screening experiments. This observation is in accordance to similar homology model-based virtual screening studies.[33] Like other knowledge-based scoring functions, PMF-Score is a relatively "soft" scoring function and performs well even in cases where the binding site geometry is not perfect.[96] The IFS produced the best result overall with a mean enrichment factor of $6.31 \pm 0.6$. This result, and the result obtained from using PMF-Score, was significantly better than the enrichment produced by the other scoring functions, as confirmed by paired *t*-tests.

As mentioned above, the enrichment factors were reported as mean values over the enrichment factors obtained in ten individual virtual screening experiments. We note that the individual results were normally distributed and similar to each other (Table 1). For instance, in the case of the IFS and PMF-Score, the standard deviation was approximately 10% of the mean value. This indicates that the individual enrichment factors were not largely biased by the composition of the individual screening sets.

Next we compared the performance of the scoring schemes at the top scoring 5% and 1% of the ranked database. The associated data (enrichment factors) are shown in Table 2 and Table 3, respectively. Again, the IFS produced the best results overall with mean enrichment factors of $8.03 \pm 1.58$ and $23.56 \pm 5.74$, for levels of 5% and 1%, respectively. At 1%, none of the conventional scoring functions produced enrichments significantly better than random. Thus, in Table 3 only enrichment factors obtained using the IFS-based scoring scheme were reported. At 5%, out of the conventional

scoring schemes, only the PMF-Score function produced results with a mean enrichment factor better than 2 ($2.12 \pm 0.52$). In practical applications, an enrichment factor of approximately 2 for the top 5% of the ranked database would be too low. Only IFS-based scoring is shown to result in enrichment factors good enough for practical virtual screening applications.

The lowest enrichment of active compounds was found for the Gold-Score function. In part, this might be explained by the fact that Gold-Score performs poorly when hydrophobic interactions are predominant,[97] as it was found for the mGluR5 binding pocket. Another reason for the low performance of the conventional scoring functions that were applied for rescoring of FlexX generated poses might be the fact that we did not perform a local *optimization* of the docking solutions with respect to the new objective functions. This procedure was shown to have a positive effect on the rescoring performance using the GOLD docking engine.[98] However, optimization with respect to the rescoring function was not possible within the CScore module of Sybyl used in this study. *Minimization* of docking poses with respect to an external molecular mechanics forcefield followed by rescoring using the native scoring function was also shown to result in improved enrichment in virtual screening experiments.[97,98] However, a similar study using FlexX and CScore reported that the relative performance of rescoring scoring functions was not affected by this procedure.[99] Therefore, and due to the additional computational costs that might render minimization an unpractical option for virtual screening of large data sets, minimization was not further investigated in this study. Local optimization or minimization prior to rescoring might have been particular important in the case of the "hard" scoring functions (ChemScore, DockScore, and Gold-Score), thus the results obtained with these scoring functions should be regarded with caution.

One additional reason for the better performance of IFP over generic scoring functions might be that poses were guided to bind to the desired part of the potential binding site, whereas this was not true for unguided scoring functions. We tried to estimate the impact of this effect by posing constraints on individual interactions from the interaction fingerprint of the reference ligands used for IFP scoring. Poses that had the required interaction (poses guided toward the correct binding site) were further ranked by the FlexX scoring function; otherwise a score of 0 was assigned. Two residues were selected for this experiment (R647 and W784) that interacted with the aligned ligands from the extracellular and intracellular side of the binding site, respectively. As expected, a large number of poses was discarded by assigning a score of 0. However, a closer examination revealed that not only true negatives were discarded but also a large number of false negatives, i.e., poses docked into the binding site that did not satisfy the pharmacophoric constrain. As a consequence, the performance of pharmacophoric restraint scoring within the top scoring 25% of the molecules did not significantly differ from the results obtained with FlexX-Score, as expressed by the enrichment factors of the top-scored 5 and 10% of the ranked database (R647: $EF_{5\%} = 1.07 \pm 0.35$, $EF_{10\%} = 0.54 \pm 0.17$; W784: $EF_{5\%} = 0.6 \pm 0.5$, $EF_{10\%} = 0.3 \pm 0.25$; FlexX-Score: $EF_{5\%} = 1.33 \pm 0.63$, $EF_{10\%} = 1.77 \pm 0.32$). The application of the simple guided docking scoring functions bore no advantage over the conventional scoring function in regard to the top scoring 25% of the molecules.

**Discriminatory Power of the Target-Biased Scoring Scheme.** To further quantify the potential of our target-biased scoring scheme, we analyzed the ability of IFS to discriminate between active and inactive compounds. In Figure 6 the distributions of the scores (the "score spectra") are shown for the active and inactive compounds. Distributions were calculated using *all* active and inactive compounds. In an ideal case, a score spectrum would consist of two well-separated, infinitely narrow peaks, for the active and the inactive compounds, respectively. More realistically are the results shown in Figure 6. Here, the score distributions were found to be relatively broad.

The score spectrum of the IFS shows a peak at 0 and a broad tail at relatively low values. The peak at 0 reflects the number of compounds that virtually have not been accommodated within the binding site. The broad tail of the distribution of the IFS reflects a number of compounds docking very poorly, i.e., compounds that were not well accommodated within the enclosed binding pocket and therefore had a low interaction fingerprint similarity to the reference ligands. Similar results were found for the distributions of the conventional scores. The compounds were again broadly distributed.

Intuitively, the more of the variance within the total data set (active *and* inactive compounds) is explained by the scoring function, the better is the discriminatory power of the scoring function. A visual inspection of the score spectra indicates that the conventional scoring functions discriminated worse between active and inactive compounds than the IFS. Recently, Seifert introduced a method to quantify this observation by using analysis of variances (ANOVA).[83] Briefly, the discriminatory power of a scoring function is assessed by measuring the coefficient $\eta^2$. By definition, $\eta^2$ is computed as between-groups sum of squares (which describes the variability in the data set due to the scoring function) divided by the total sum of squares (which measures the overall variability). Just as the correlation coefficient $r^2$ is interpreted as the percent of variance in one variable explained by another variable, the parameter $\eta^2$ can be interpreted as the percent of variance in the actual data set explained by the scoring function.

According to the ANOVA analysis, the IFS-based scoring was able to discriminate significantly between the known actives and the inactive compounds ($\eta^2 = 13.45\%$) (Table 4). In the case of PMF-Score, FlexX-Score, ChemScore, Dock-Score, and Gold-Score, the discriminatory power was significant but much lower than in the case of the IFS. In all cases, significance was affirmed by the traditional $F$-ratio. As stated above, results obtained with ChemScore, Dock-Score, and Gold-Score should be regarded with caution. To put the ANOVA results into proper perspective, we note that $\eta^2$ values between 9% and 16% have been obtained for docking a database against a crystal structure.[83] Interestingly, the best discrimination between active and inactive molecules out of the conventional scoring functions was achieved by using ChemScore. This fact was obscured from simply looking at the enrichment curve (Figure 5).

The discriminatory power of the scoring functions was also compared to the discriminatory power of physicochemical properties, such as the molecular weight in Da or the

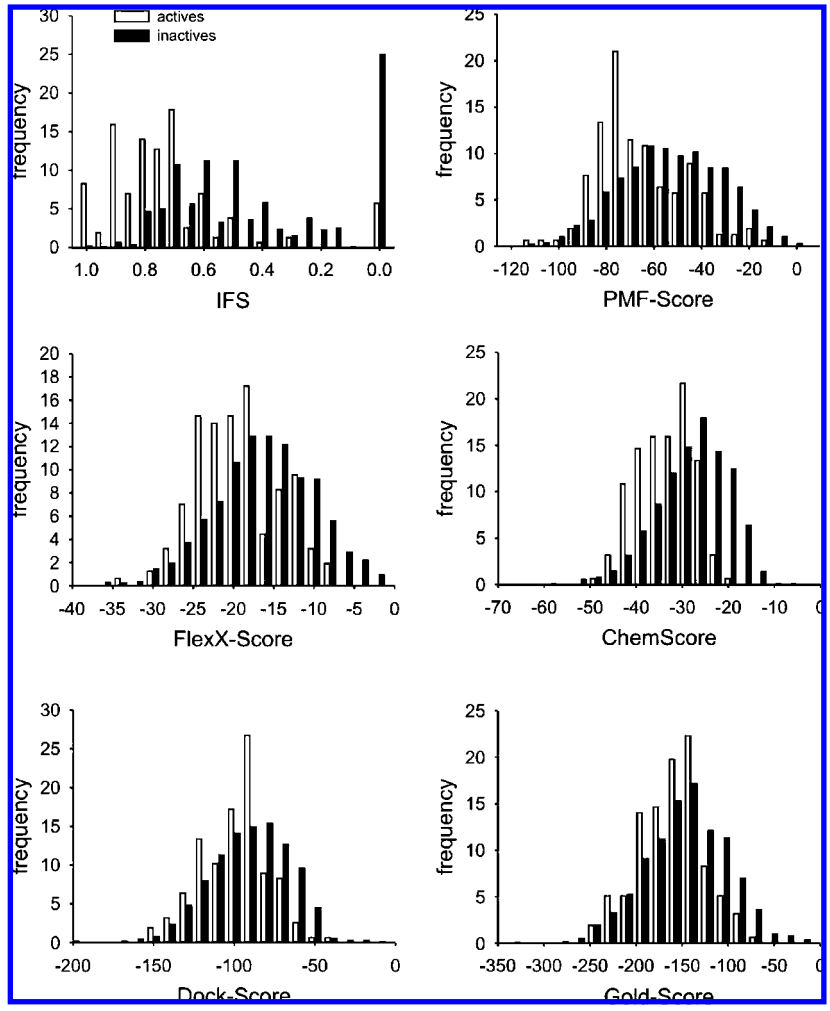


**Figure 6.** Score distributions ("score spectra") for the set of active compounds and the inactive compounds. Distributions are shown for the IFS, PMF-Score, FlexX-Score, ChemScore, Dock-Score, and Gold-Score. All active and inactive compounds were taken into account.

**Table 4.** ANOVA Results for the Distributions of the IFS and the Conventional Scores

| | $\eta^2$ | $F$ |
|---|---|---|
| IFS | 13.45 | 227.29 |
| PMF-Score | 2.71 | 51.75 |
| FlexX-Score | 2.15 | 41.98 |
| ChemScore | 4.30 | 83.86 |
| Dock-Score | 0.72 | 13.49 |
| Gold-Score | 0.76 | 14.18 |

ratio of rotatable bonds to the total number of bonds (see the Methods section). Interestingly, the discriminatory power of the conventional scoring functions was in the same range as the discriminatory power of the physicochemical properties, with $\eta^2$ values varying from 0.5 to 4.3%.

To understand, why the conventional scoring functions discriminate worse between active and inactive compounds, we examined the dependency of the score of a compound from its size. It is a well-known fact that conventional scoring functions tend to disfavor smaller molecules.[96]

In Figure 7, scatter plots of the score versus the molecular weight are shown for the set of active compounds. These plots allow inspection of the characteristics of the compounds that score better than others. The result obtained from using the IFS-based scoring scheme was not biased toward the molecular weight of the compounds. However, in the case of the PMF-Score function, a cluster of low molecular weight compounds was identified that scored low. This effect has been previously observed by Muegge and Martin.[100] Smaller compounds (<250 Da) obtained a mean score of $-61.3 \pm 17.7$, whereas the mean score of the larger compounds was significantly smaller ($-72.0 \pm 18.1$), as affirmed by a paired $t$-test. The means of the two subpopulations can also be identified in the distribution plot of the PMF-Score (Figure 6).

Similar observations were made in the case of the other conventional scoring functions (data not shown). Remarkably, when the IFS was used, the results were not biased due to the molecular weight of the compounds in the screening set, i.e, there was no significant difference between the mean IFS of the smaller compounds and the mean IFS of the larger compounds. Thus, the IFS-based scoring scheme improved the results and was allowed to incorporate implicitly the adaptivity of the receptor binding site to different sizes of ligands.

**Dependence of the Discriminatory Power on the Reference Compounds.** The results from the previous paragraphs show that the enrichment of GPCR ligands and the discrimination between active and inactive compounds can significantly be improved by including relevant ligand-based information into the homology modeling and scoring process. However, enrichment is a measure of performance that asks how quickly active compounds are found. It is not

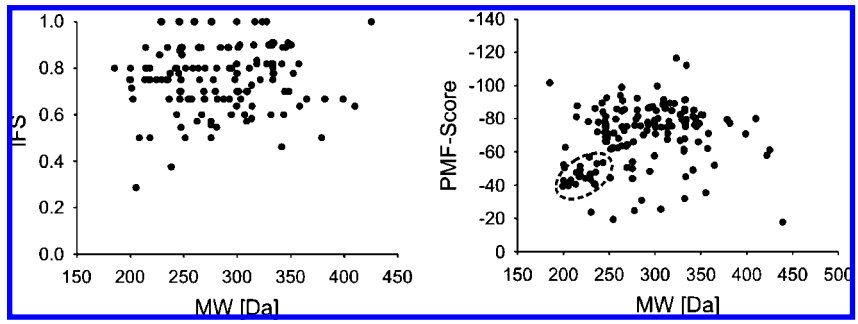


**Figure 7.** Scatter plots of the score versus the molecular weight, for the set of active compounds. Plots are shown for the IFS-based scoring scheme and the PMF-Score function. In the plot for the PMF-Score function, a cluster of low molecular weight compounds that score low is accentuated by the circle. All active compounds were taken into account. In the case of the target-biased scoring scheme, compounds with an IFS of 0 were discarded.

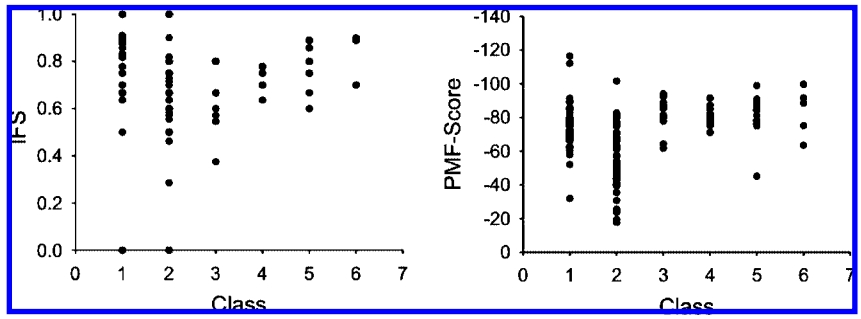


**Figure 8.** Score distributions ("score spectra") of the active compounds from the six different scaffold classes (1: MPEP/MTEP derivatives, 2: tetrazole pyridines, 3: dipyridyl amides, 4: thiopyrimidines, 5: phenyl ureas, 6: benzoxazoles). Distributions are shown for the IFS and PMF-Score. All active compounds were taken into account.

a measure of diversity or completeness. While finding active leads rapidly is important in practical application of these algorithms toward virtual screening, an equally important measure of algorithm robustness is the ability to identify *structurally diverse* leads.

As in the case of the IFS-based scoring function, a couple of schemes exist that allow for the incorporation of additional information into the docking process. Often, a small number of specific intermolecular constraints is imposed, e.g., by using a combined 3D receptor- and ligand-based pharmacophore hypothesis. A typical three- or four-point pharmacophore will be too restrictive and yield few interesting hits, whereas a slightly more open-ended query may yield too many hits. Furthermore, the application of such schemes may limit the diversity of potential ligands evaluated to a subset of the total collection, which may be undesirable when maximal diversity of drug leads is sought. A similar effect is observed when ligand-based information is exploited using substructure fingerprints like Unity[101] and Daylight[102] fingerprints or MACCS keys.[103] These methods produce high enrichment rates; they tend, however, to predict structures whose scaffolds are already present in the set of reference compounds.[18,19]

In the development of the IFS-based scoring scheme presented here, ligand-based information was not incorporated by imposing a small number of intermolecular (pharmacophore) constraints or by using substructure fingerprints. Instead, a large number of weak (residue-based) ligand−receptor interaction restraints were incorporated. In the case of mGluR5, the interaction fingerprints encoded for 53 potential interactions with the binding site. Information about the type and the strength of the interaction was discarded. It was not required that a screening compound obeyed all interaction restraints. It was only important that the interaction pattern of the compound was somehow similar to one of the interaction patterns of the reference compounds.

However, incorporating ligand-based information into the virtual screening process naturally biases the outcome toward the reference compounds. To test the strength of this dependence, we compared the score spectra of the active compounds from the six different scaffold classes. The scaffold classes comprised in the set of active compounds were MPEP/MTEP derivatives, tetrazole pyridines, dipyridyl amides, thiopyrimidines, phenyl ureas, and benzoxazoles. Among the five reference compounds (Figure 2) were three tetrazole pyridines (compounds **1**, **2**, and **3**) and two MPEP/MTEP derivatives (compounds **4** and **5**). The remaining scaffold classes were not contained in the reference set.

In Figure 8, score spectra of the active compounds from the six different scaffold classes are shown. The distributions of the IFS are compared to the distributions of the PMF-Score. Not surprisingly, IFS was slightly biased toward the scaffold classes that were included in the set of reference ligands, as can be seen from the fact that IFS values of 1 were obtained for tetrazole pyridines and MPEP/MTEP derivatives. However, also for the compounds of the remaining scaffolds rather high IFS values (up to >0.9) were obtained. This result demonstrates the scaffold hopping ability with the IFS-based scoring scheme, at least within the current screening set. This observation might be explained by the fact that the reference ligands were rather dissimilar with respect to their potential patterns of interactions with the receptor binding site (although structurally similar).

When the PMF-Score function was used, best (negative) scores were obtained for tetrazole pyridines (Figure 8). Overall, the compounds of all scaffold classes were scored

equally well, with the exemption of the MPEP/MTEP derivatives. The latter were scored significantly worse compared to the compounds of the remaining scaffold classes. This might have been due to the fact that MPEP/MTEP derivatives have a relatively low molecular weight. As described above, conventional scoring functions prioritize large compounds.

## CONCLUSION

In the present study, the combination of two recently reported techniques for the improvement of homology model-based virtual screening for GPCR ligands was investigated. In the first step, ligand-supported homology modeling was applied. Clues to infer the binding modes of the ligands were provided by data from mutagenesis studies. In the second step, to rank order docking solutions, a scoring scheme was developed that exploits the patterns of interactions between ligands already known to bind to the target and the binding site. As reference ligands, the compounds that have already been employed to support homology modeling were used. Patterns of interactions were modeled using binary ligand−receptor fingerprints (analogous to the SIFt structural interaction fingerprint approach).

We validated our approach in retrospective virtual screening experiments against the metabotropic glutamate receptor (mGluR) subtype 5. To put the results into proper perspective, docking solutions were also rank ordered using conventional scoring functions (Dock-Score, PMF-Score, Gold-Score, ChemScore, and FlexX-Score). To the best of our knowledge, no homology model-based virtual screening against the mGluR5 has been carried out. The mGluR5 represents a challenging system due to the occurrence of large nonpolar regions in the binding pocket.

Using the IFS, enrichment rates could significantly be improved. We showed that the power of the IFS to discriminate between active and inactive compounds was superior to the discriminatory power of conventional scoring functions. Though using a target-biased scoring approach, the results were not biased toward the chemical classes of the reference structures. Moreover, we demonstrated that the IFS-based scoring function was not biased toward compounds of relatively high molecular weight, as it has been observed for the conventional scoring function, or toward the reference compounds. Finally, the number of CPU cycles required when using the target-biased scoring scheme was not significantly higher compared to the cycles required when using conventional scoring functions for rank ordering the compounds.

Considering the success of our scoring methodology, we expect the presented approach to serve as a general setup for successful GPCR virtual screening. The approach bears a high potential for the analyses and interpretation of the binding modes of ligands of the metabotropic glutamate receptor family and might allow an assessment of the selectivity profile of individual ligands.

## ACKNOWLEDGMENT

We thank Gabriele Costantino and Gisbert Schneider for valuable discussions regarding the mGluR5 homology model and Swetlana Derksen for the interaction fingerprint code.

**Supporting Information Available:** Details on the calculation of the homology model and on the analysis of the virtual screening results and the set of active ligands used for virtual screening. This material is available free of charge via the Internet at http://pubs.acs.org.

## REFERENCES AND NOTES

(1) Hopkins, A. L.; Groom, C. R. The druggable genome. *Nat. Rev. Drug Discovery* **2002**, *1*, 727–730.
(2) Klabunde, T.; Hessler, G. Drug design strategies for targeting G-protein-coupled receptors. *ChemBioChem* **2002**, *3*, 929–944.
(3) Schlyer, S.; Horuk, R. I want a new drug: G-protein-coupled receptors in drug development. *Drug Discovery Today* **2006**, *11*, 481–493.
(4) Swanson, C. J.; Bures, M.; Johnson, M. P.; Linden, A. M.; Monn, J. A.; Schoepp, D. D. Metabotropic glutamate receptors as novel targets for anxiety and stress disorders. *Nat. Rev. Drug Discovery* **2005**, *4*, 131–134.
(5) Noeske, T.; Gutcaits, A.; Parsons, C. G.; Weil, T. Allosteric modulation of family 3 GPCRs. *QSAR Comb. Sci.* **2006**, *25*, 134–146.
(6) Palczewski, K.; Kumasaka, T.; Hori, T.; Behnke, C. A.; Motoshima, H.; Fox, B. A.; Le Trong, I.; Teller, D. C.; Okada, T.; Stenkamp, R. E.; Yamamoto, M.; Miyano, M. Crystal structure of rhodopsin: A G protein-coupled receptor. *Science* **2000**, *289*, 739–745.
(7) Teller, D. C.; Okada, T.; Behnke, C. A.; Palczewski, K.; Stenkamp, R. E. Advances in determination of a high-resolution three-dimensional structure of rhodopsin, a model of G-protein-coupled receptors (GPCRs). *Biochemistry* **2001**, *40*, 7761–7772.
(8) Shacham, S.; Marantz, Y.; Bar-Haim, S.; Kalid, O.; Warshaviak, D.; Avisar, N.; Inbal, B.; Heifetz, A.; Fichman, M.; Topf, M.; Naor, Z.; Noiman, S.; Becker, O. M. PREDICT modeling and in-silico screening for G-protein coupled receptors. *Proteins* **2004**, *57*, 51–86.
(9) Becker, O. M.; Shacham, S.; Marantz, Y.; Noiman, S. Modeling the 3D structure of GPCRs: Advances and application to drug discovery. *Curr. Opin. Drug Discovery Dev.* **2003**, *6*, 353–361.
(10) Trabanino, R. J.; Hall, S. E.; Vaidehi, N.; Floriano, W. B.; Kam, V. W. T.; Goddard, W. A. First principles predictions of the structure and function of G-protein-coupled receptors: Validation for bovine rhodopsin. *Biophys. J.* **2004**, *86*, 1904–1921.
(11) Vaidehi, N.; Floriano, W. B.; Trabanino, R.; Hall, S. E.; Freddolino, P.; Choi, E. J.; Zamanakos, G.; Goddard, W. A. Prediction of structure and function of G protein-coupled receptors. *Proc. Natl. Acad. Sci. U.S.A.* **2002**, *99*, 12622–12627.
(12) Cherezov, V.; Rosenbaum, D. M.; Hanson, M. A.; Rasmussen, S. G. F.; Thian, F. S.; Kobilka, T. S.; Choi, H. J.; Kuhn, P.; Weis, W. I.; Kobilka, B. K.; Stevens, R. C. High-resolution crystal structure of an engineered human beta(2)-adrenergic G protein-coupled receptor. *Science* **2007**, *318*, 1258–1265.
(13) Bender, A.; Glen, R. C. Molecular similarity: a key technique in molecular informatics. *Org. Biomol. Chem.* **2004**, *2*, 3204–3218.
(14) Marriott, D. P.; Dougall, I. G.; Meghani, P.; Liu, Y. J.; Flower, D. R. Lead generation using pharmacophore mapping and three-dimensional database searching: Application to muscarinic M-3 receptor antagonists. *J. Med. Chem.* **1999**, *42*, 3210–3216.
(15) Flohr, S.; Kurz, M.; Kostenis, E.; Brkovich, A.; Fournier, A.; Klabunde, T. Identification of nonpeptidic urotensin II receptor antagonists by virtual screening based on a pharmacophore model derived from structure-activity relationships and nuclear magnetic resonance studies on urotensin II. *J. Med. Chem.* **2002**, *45*, 1799–1805.
(16) Renner, S.; Noeske, T.; Parsons, C. G.; Schneider, P.; Weil, T.; Schneider, G. New allosteric modulators of metabotropic glutamate receptor 5 (mGluR5) found by ligand-based virtual screening. *ChemBioChem* **2005**, *6*, 620–625.
(17) Renner, S.; Hechenberger, M.; Noeske, T.; Bocker, A.; Jatzke, C.; Schmuker, M.; Parsons, C. G.; Weil, T.; Schneider, G. Searching for Drug Scaffolds with 3D Pharmacophores and Neural Network Ensembles. *Angew. Chem., Int. Ed.* **2007**, *46*, 5336–5339.
(18) Schneider, G.; Schneider, P.; Renner, S. Scaffold-hopping: How far can you jump. *QSAR Comb. Sci.* **2006**, *25*, 1162–1171.
(19) Zhang, Q.; Muegge, I. Scaffold hopping through virtual screening using 2D and 3D similarity descriptors: Ranking, voting, and consensus scoring. *J. Med. Chem.* **2006**, *49*, 1536–1548.
(20) Sheridan, R. P. Chemical similarity searches: when is complexity justified. *Expert Opin. Drug Discovery* **2007**, *2*, 423–430.
(21) Renner, S.; Schneider, G. Scaffold-hopping potential of ligand-based similarity concepts. *ChemMedChem* **2006**, *1*, 181–185.
(22) Kitchen, D. B.; Decornez, H.; Furr, J. R.; Bajorath, J. Docking and scoring in virtual screening for drug discovery: Methods and applications. *Nat. Rev. Drug Discovery* **2004**, *3*, 935–949.

(23) Lyne, P. D. Structure-based virtual screening: an overview. *Drug Discovery Today* **2002**, *7*, 1047–1055.
(24) Congreve, M.; Murray, C. W.; Blundell, T. L. Keynote review: Structural biology and drug discovery. *Drug Discovery Today* **2005**, *10*, 895–907.
(25) Gohlke, H.; Klebe, G. Approaches to the Description and Prediction of the Binding Affinity of Small-Molecule Ligands to Macromolecular Receptors. *Angew. Chem., Int. Ed.* **2002**, *41*, 2644–2676.
(26) Evers, A.; Klebe, G. Successful virtual screening for a submicromolar antagonist of the neurokinin-1 receptor based on a ligand-supported homology model. *J. Med. Chem.* **2004**, *47*, 5381–5392.
(27) Bissantz, C.; Logean, A.; Rognan, D. High-throughput modeling of human G-protein coupled receptors: Amino acid sequence alignment, three-dimensional model building, and receptor library screening. *J. Chem. Inf. Comput. Sci.* **2004**, *44*, 1162–1176.
(28) Bissantz, C.; Bernard, P.; Hibert, M.; Rognan, D. Protein-based virtual screening of chemical databases. II. Are homology models of G-protein coupled receptors suitable targets. *Proteins* **2003**, *50*, 5–25.
(29) Becker, O. M.; Marantz, Y.; Shacham, S.; Inbal, B.; Heifetz, A.; Kalid, O.; Bar-Haim, S.; Warshaviak, D.; Fichman, M.; Noiman, S. G protein-coupled receptors: In silico drug discovery in 3D. *Proc. Natl. Acad. Sci. U.S.A.* **2004**, *101*, 11304–11309.
(30) Varady, J.; Wu, X. H.; Fang, X. L.; Min, J.; Hu, Z. J.; Levant, B.; Wang, S. M. Molecular modeling of the three-dimensional structure of dopamine 3 (D-3) subtype receptor: Discovery of novel and potent D-3 ligands through a hybrid pharmacophore- and structure-based database searching approach. *J. Med. Chem.* **2003**, *46*, 4377–4392.
(31) Hobrath, J. V.; Wang, S. M. Computational elucidation of the structural basis of ligand binding to the dopamine 3 receptor through docking and homology modeling. *J. Med. Chem.* **2006**, *49*, 4470–4476.
(32) Evers, A.; Klabunde, T. Structure-based drug discovery using GPCR homology modeling: Successful virtual screening for antagonists of the Alpha1A adrenergic receptor. *J. Med. Chem.* **2005**, *48*, 1088–1097.
(33) Evers, A.; Hessler, G.; Matter, H.; Klabunde, T. Virtual screening of biogenic amine-binding G-protein coupled receptors: Comparative evaluation of protein- and ligand-based virtual screening protocols. *J. Med. Chem.* **2005**, *48*, 5448–5465.
(34) McGovern, S. L.; Shoichet, B. K. Information decay in molecular docking screens against holo, apo, and modeled conformations of enzymes. *J. Med. Chem.* **2003**, *46*, 2895–2907.
(35) Bindewald, E.; Skolnick, J. A scoring function for docking ligands to low-resolution protein structures. *J. Comput. Chem.* **2005**, *26*, 374–383.
(36) Evers, A.; Gohlke, H.; Klebe, G. Ligand-supported homology modelling of protein binding sites using knowledge-based potentials. *J. Mol. Biol.* **2003**, *334*, 327–345.
(37) Seifert, M. H. J.; Kraus, J.; Kramer, B. Virtual high-throughput screening of molecular databases. *Curr. Opin. Drug Discovery Dev.* **2007**, *10*, 298–307.
(38) Fradera, X.; Mestres, J. Guided docking approaches to structure-based design and screening. *Curr. Top. Med. Chem.* **2004**, *4*, 687–700.
(39) Jansen, J. M.; Martin, E. J. Target-biased scoring approaches and expert systems in structure-based virtual screening. *Curr. Opin. Chem. Biol.* **2004**, *8*, 359–364.
(40) Hindle, S. A.; Rarey, M.; Buning, C.; Lengauer, T. Flexible docking under pharmacophore type constraints. *J. Comput.-Aided Mol. Des.* **2002**, *16*, 129–149.
(41) Fradera, X.; Knegtel, R. M.; Mestres, J. Similarity-driven flexible ligand docking. *Proteins* **2000**, *40*, 623–636.
(42) Daeyaert, F.; de Jonge, M.; Heeres, J.; Koymans, L.; Lewi, P.; Vinkers, M. H.; Janssen, P. A. J. A pharmacophore docking algorithm and its application to the cross-docking of 18 HIV-NNRTI's in their binding pockets. *Proteins* **2004**, *54*, 526–533.
(43) Wu, G. S.; Vieth, M. SDOCKER: A method utilizing existing X-ray structures to improve docking accuracy. *J. Med. Chem.* **2004**, *47*, 3142–3148.
(44) Radestock, S.; Böhm, M.; Gohlke, H. Improving binding mode predictions by docking into protein-specifically adapted potential fields. *J. Med. Chem.* **2005**, *48*, 5466–5479.
(45) Renner, S.; Derksen, S.; Radestock, S.; Mörchen, F. Maximum common binding modes (MCBM): Consensus docking scoring using multiple ligand information and interaction fingerprints. *J. Chem. Inf. Model.* **2008**, *48*, 319–332.
(46) Deng, Z.; Chuaqui, C.; Singh, J. Structural interaction fingerprint (SIFt): A novel method for analyzing three-dimensional protein-ligand binding interactions. *J. Med. Chem.* **2004**, *47*, 337–344.
(47) Kelly, M. D.; Mancera, R. L. Expanded interaction fingerprint method for analyzing ligand binding modes in docking and structure-based drug design. *J. Chem. Inf. Comput. Sci.* **2004**, *44*, 1942–1951.
(48) Mpamhanga, C. P.; Chen, B. N.; McLay, I. M.; Willett, P. Knowledge-based interaction fingerprint scoring: A simple method for improving the effectiveness of fast scoring functions. *J. Chem. Inf. Model.* **2006**, *46*, 686–698.
(49) Spooren, W. P. J. M.; Gasparini, F.; Salt, T. E.; Kuhn, R. Novel allosteric antagonists shed light on mglu(5) receptors and CNS disorders. *Trends Pharmacol. Sci.* **2001**, *22*, 331–337.
(50) Rarey, M.; Kramer, B.; Lengauer, T.; Klebe, G. A fast flexible docking method using an incremental construction algorithm. *J. Mol. Biol.* **1996**, *261*, 470–489.
(51) Willett, P.; Barnard, J. M.; Downs, G. M. Chemical similarity searching. *J. Chem. Inf. Comput. Sci.* **1998**, *38*, 983–996.
(52) Malherbe, P.; Kratochwil, N.; Zenner, M. T.; Piussi, J.; Diener, C.; Kratzeisen, C.; Fischer, C.; Porter, R. H. P. Mutational analysis and molecular modeling of the binding pocket of the metabotropic glutamate 5 receptor negative modulator 2-methyl-6-(phenylethynyl)-pyridine. *Mol. Pharmacol.* **2003**, *64*, 823–832.
(53) Pagano, A.; Ruegg, D.; Litschig, S.; Stoehr, N.; Stierlin, C.; Heinrich, M.; Floersheim, P.; Prezeau, L.; Carroll, F.; Pin, J. P.; Cambria, A.; Vranesic, I.; Flor, P. J.; Gasparini, F.; Kuhn, R. The non-competitive antagonists 2-methyl-6-(phenylethynyl)pyridine and 7-hydroxyiminocyclopropan[b]chromen-1 alpha-carboxylic acid ethyl ester interact with overlapping binding pockets in the transmembrane region of group I metabotropic glutamate receptors. *J. Biol. Chem.* **2000**, *275*, 33750–33758.
(54) Malherbe, P.; Kratochwil, N.; Mühlemann, A.; Zenner, M. T.; Fischer, C.; Stahl, M.; Gerber, P. R.; Jaeschke, G.; Porter, R. H. P. Comparison of the binding pockets of two chemically unrelated allosteric antagonists of the mGlu5 receptor and identification of crucial residues involved in the inverse agonism of MPEP. *J. Neurochem.* **2006**, *98*, 601–615.
(55) Mühlemann, A.; Ward, N. A.; Kratochwil, N.; Diener, C.; Fischer, C.; Stucki, A.; Jaeschke, G.; Malherbe, P.; Porter, R. H. P. Determination of key amino acids implicated in the actions of allosteric modulation by 3,3′-difluorobenzaldazine on rat mGlu5 receptors. *Eur. J. Pharmacol.* **2006**, *529*, 95–104.
(56) Surgand, J. S.; Rodrigo, J.; Kellenberger, E.; Rognan, D. A chemogenomic analysis of the transmembrane binding cavity of human G-protein-coupled receptors. *Proteins* **2006**, *62*, 509–538.
(57) Kratochwil, N. A.; Malherbe, P.; Lindemann, L.; Ebeling, M.; Hoener, M. C.; Muhlemann, A.; Porter, R. H. P.; Stahl, M.; Gerber, P. R. An automated system for the analysis of G protein-coupled receptor transmembrane binding pockets: Alignment, receptor-based pharmacophores, and their application. *J. Chem. Inf. Model.* **2005**, *45*, 1324–1336.
(58) Huang, D. H.; Poon, S. F.; Chapman, D. F.; Chung, J.; Cramer, M.; Reger, T. S.; Roppe, J. R.; Tehrani, L.; Cosford, N. D. P.; Smith, N. D. 2-{2-[3-(pyridin-3-yloxy)phenyl]-2H-tetrazol-5-yl}pyridine: a highly potent, orally active, metabotropic glutamate subtype 5 (mGlu5) receptor antagonist. *Bioorg. Med. Chem. Lett.* **2004**, *14*, 5473–5476.
(59) Eastman, B.; Chen, C. X.; Smith, N. D.; Poon, S.; Chung, J.; Reyes-Manalo, G.; Cosford, N. D. P.; Munoz, B. Expedited SAR study of an mGluR5 antagonists: generation of a focused library using a solution-phase Suzuki coupling methodology. *Bioorg. Med. Chem. Lett.* **2004**, *14*, 5485–5488.
(60) Poon, S. F.; Eastman, B. W.; Chapman, D. F.; Chung, J.; Cramer, M.; Holtz, G.; Cosford, N. D. P.; Smith, N. D. 3-[3-fluoro-5-(5-pyridin-2-yl-2H-tetrazol-2-yl)phenyl]-4-methylpyridine: a highly potent and orally bioavailable metabotropic glutamate subtype 5 (mGlu5) receptor antagonist. *Bioorg. Med. Chem. Lett.* **2004**, *14*, 5477–5480.
(61) Roppe, J.; Smith, N. D.; Huang, D. H.; Tehrani, L.; Wang, B. W.; Anderson, J.; Brodkin, J.; Chung, J.; Jiang, X. H.; King, C.; Munoz, B.; Varney, M. A.; Prasit, P.; Cosford, N. D. P. Discovery of novel heteroarylazoles that are metabotropic glutamate subtype 5 receptor antagonists with anxiolytic activity. *J. Med. Chem.* **2004**, *47*, 4645–4648.
(62) Smith, N. D.; Poon, S. F.; Huang, D. H.; Green, M.; King, C.; Tehrani, L.; Roppe, J. R.; Chung, J.; Chapman, D. P.; Cramer, M.; Cosford, N. D. P. Discovery of highly potent, selective, orally bioavailable, metabotropic glutamate subtype 5 (mGlu5) receptor antagonists devoid of cytochrome P450 1A2 inhibitory activity. *Bioorg. Med. Chem. Lett.* **2004**, *14*, 5481–5484.
(63) Varney, M. A.; Cosford, N. D. P.; Jachec, C.; Rao, S. P.; Sacaan, A.; Lin, F. F.; Bleicher, L.; Santori, E. M.; Flor, P. J.; Allgeier, H.; Gasparini, F.; Kuhn, R.; Hess, S. D.; Velicelebi, G.; Johnson, E. C. SIB-1757 and SIB-1893: Selective, noncompetitive antagonists of metabotropic glutamate receptor type 5. *J. Pharmacol. Exp. Ther.* **1999**, *290*, 170–181.
(64) Molecular Operation Environment, Chemical Computing Group, Inc., Montreal, Quebec, Canada, 2006.

(65) Noeske, T.; Jirgensons, A.; Starchenkovs, I.; Renner, S.; Jaunzeme, I.; Trifanova, D.; Hechenberger, M.; Bauer, T.; Kauss, V.; Parsons, C. G.; Schneider, G.; Weil, T. Virtual Screening for Selective Allosteric mGluR1 Antagonists and Structure-Activity Relationship Investigations for Coumarine Derivatives. *ChemMedChem* **2007**, 1763–1773.

(66) Vanejevs, M.; Jatzke, C.; Renner, S.; Müller, S.; Hechenberger, M.; Bauer, T.; Klochkova, A.; Pyatkin, I.; Kazyulkin, D.; Aksenova, E.; Shulepin, S.; Timonina, O.; Haasis, A.; Gutcaits, A.; Parson, C. G.; Kauss, V.; Weil, T. Positive and Negative Modulation of Group I Metabotropic Glutamate Receptors. *J. Med. Chem.* **2007**, *51*, 634–647.

(67) Sybyl Molecular Modeling Software, 7.2; Tripos Inc., St. Louis, MO, 2006.

(68) Ballesteros, J. A.; Shi, L.; Javitch, J. A. Structural mimicry in G protein-coupled receptors: Implications of the high-resolution structure of rhodopsin for structure-function analysis of rhodopsin-like receptors. *Mol. Pharmacol.* **2001**, *60*, 1–19.

(69) Alagille, D.; Baldwin, R. M.; Roth, B. L.; Wroblewski, J. T.; Grajkowska, E.; Tamagnan, G. D. Functionalization at position 3 of the phenyl ring of the potent mGluR5 noncompetitive antagonists MPEP. *Bioorg. Med. Chem. Lett.* **2005**, *15*, 945–949.

(70) Bonnefous, C.; Vernier, J. M.; Hutchinson, J. H.; Chung, J.; Reyes-Manalo, G.; Kamenecka, T. Dipyridyl amides: potent metabotropic glutamate subtype 5 (mGlu5) receptor antagonists. *Bioorg. Med. Chem. Lett.* **2005**, *15*, 1197–1200.

(71) Cosford, N. D. P.; Tehrani, L.; Roppe, J.; Schweiger, E.; Smith, N. D.; Anderson, J.; Bristow, L.; Brodkin, J.; Jiang, X. H.; McDonald, I.; Rao, S.; Washburn, M.; Varney, M. A. 3-[(2-methyl-1,3-thiazol-4-yl)ethynyl]pyridine: A potent and highly selective metabotropic glutamate subtype 5 receptor antagonist with anxiolytic activity. *J. Med. Chem.* **2003**, *46*, 204–206.

(72) Iso, Y.; Grajkowska, E.; Wroblewski, J. T.; Davis, J.; Goeders, N. E.; Johnson, K. M.; Sanker, S.; Roth, B. L.; Tueckmantel, W.; Kozikowski, A. P. Synthesis and structure-activity relationships of 3-[(2-methyl-1,3-thiazol-4-yl)ethynyl]pyridine analogues as potent, noncompetitive metabotropic glutamate receptor subtype 5 antagonists; Search for cocaine medications. *J. Med. Chem.* **2006**, *49*, 1080–1100.

(73) Roppe, J. R.; Wang, B. W.; Huang, D. H.; Tehrani, L.; Kamenecka, T.; Schweiger, E. J.; Anderson, J. J.; Brodkin, J.; Jiang, X. H.; Cramer, M.; Chung, J.; Reyes-Manalo, G.; Munoz, B.; Cosford, N. D. P. 5-[(2-methyl-1,3-thiazol-4-yl)ethynyl]-2,3′-bipyridine: a highly potent, orally active metabotropic glutamate subtype 5 (mGlu5) receptor antagonist with anxiolytic activity. *Bioorg. Med. Chem. Lett.* **2004**, *14*, 3993–3996.

(74) Wallberg, A.; Nilsson, K.; Osterlund, K.; Peterson, A.; Elg, S.; Raboisson, P.; Bauer, U.; Hammerland, L. G.; Mattsson, J. P. Phenyl ureas of creatinine as mGluR5 antagonists. A structure-activity relationship study of fenobam analogues. *Bioorg. Med. Chem. Lett.* **2006**, *16*, 1142–1145.

(75) Wang, B. W.; Vernier, J. M.; Rao, S.; Chung, J.; Anderson, J. J.; Brodkin, J. D.; Jiang, X. H.; Gardner, M. F.; Yang, X. Q.; Munoz, B. Discovery of novel modulators of metabotropic glutamate receptor subtype-5. *Bioorg. Med. Chem.* **2004**, *12*, 17–21.

(76) Hammerland, L. G.; Johansson, M.; Malmstrom, J.; Mattsson, J. P.; Minidis, A. B. E.; Nilsson, K.; Peterson, A.; Wensbo, D.; Wallberg, A.; Osterlund, K. Structure-activity relationship of thiopyrimidines as mGluR5 antagonists. *Bioorg. Med. Chem. Lett.* **2006**, *16*, 2467–2469.

(77) Arora, J.; Edwards, L.; Isaac, M.; Kers, A.; Staaf, K.; Slassi, A.; Stefanac, T.; Wensbo, D.; Xin, T.; Holm, B. Synthesis of polyheterocyclic compounds as metabotropic glutamate receptor antagonists. WO2005080386, 2005.

(78) Edwards, L.; Isaac, M.; Johansson, M.; Malmberg, J.; Minidis, A.; Staaf, K.; Slassi, A.; Wensbo, D. Preparation of triazoles as mGluR5 metabotropic glutamate receptor antagonists. WO2005080379, 2005.

(79) Johansson, M.; Minidis, A.; Staaf, K.; Wensbo, D.; McLeod, D.; Edwards, L.; Isaac, M.; O'Brien, A.; Slassi, A.; Xin, T. Preparation of tetrazole compounds and their use as metabotropic glutamate receptor antagonists. WO2005080356, 2005.

(80) Johansson, M.; Wensbo, D.; Minidis, A.; Staaf, K.; Kers, A.; Edwards, L.; Isaac, M.; Stefanac, T.; Slassi, A.; McLeod, D. Preparation of heterocyclic-fused 1,3-diazenes and analogs as metabotropic glutamate receptor antagonists. WO2005080397, 2005.

(81) Wensbo, D.; Edwards, L.; Isaac, M.; McLeod, D. A.; Slassi, A.; Xin, T.; Stormann, T. M. Fluoro-, chloro- and cyano-pyridin-2-yl-tetrazoles as ligands of the metabotropic glutamate receptor 5. WO2005066155, 2005.

(82) Li, C. L.; Xu, L.; Wolan, D. W.; Wilson, I. A.; Olson, A. J. Virtual screening of human 5-aminoimidazole-4-carboxamide ribonucleotide transformylase against the NCI diversity set by use of AutoDock to identify novel nonfolate inhibitors. *J. Med. Chem.* **2004**, *47*, 6681–6690.

(83) Seifert, M. H. J. Assessing the discriminatory power of scoring functions for virtual screening. *J. Chem. Inf. Model.* **2006**, *46*, 1456–1465.

(84) Halgren, T. A.; Murphy, R. B.; Friesner, R. A.; Beard, H. S.; Frye, L. L.; Pollard, W. T.; Banks, J. L. Glide: A new approach for rapid, accurate docking and scoring. 2. Enrichment factors in database screening. *J. Med. Chem.* **2004**, *47*, 1750–1759.

(85) Yang, Y.; Dickinson, C.; Haskell-Luevano, C.; Gantz, I. Molecular basis for the interaction of [Nle4,D-Phe7]melanocyte stimulating hormone with the human melanocortin-1 receptor. *J. Biol. Chem.* **1997**, *272*, 23000–23010.

(86) Betz, S. F.; Reinhart, G. J.; Lio, F. M.; Chen, C.; Struthers, R. S. Overlapping, nonidentical binding sites of different classes of nonpeptide antagonists for the human gonadotropin-releasing hormone receptor. *J. Med. Chem.* **2006**, *49*, 637–647.

(87) Gao, Z. G.; Chen, A.; Barak, D.; Kim, S. K.; Muller, C. E.; Jacobson, K. A. Identification by site-directed mutagenesis of residues involved in ligand recognition and activation of the human A3 adenosine receptor. *J. Biol. Chem.* **2002**, *277*, 19056–19063.

(88) Malherbe, P.; Kratochwil, N.; Knoflach, F.; Zenner, M. T.; Kew, J. N. C.; Kratzeisen, C.; Maerki, H. P.; Adam, G.; Mutel, V. Mutational analysis and molecular modeling of the allosteric binding site of a novel, selective, noncompetitive antagonist of the metabotropic glutamate 1 receptor. *J. Biol. Chem.* **2003**, *278*, 8340–8347.

(89) Litschig, S.; Gasparini, F.; Rueegg, D.; Stoehr, N.; Flor, P. J.; Vranesic, I.; Prezeau, L.; Pin, J. P.; Thomsen, C.; Kuhn, R. CPCCOEt, a noncompetitive metabotropic glutamate receptor 1 antagonist, inhibits receptor signaling without affecting glutamate binding. *Mol. Pharmacol.* **1999**, *55*, 453–461.

(90) Petrel, C.; Kessler, A.; Dauban, P.; Dodd, R. H.; Rognan, D.; Ruat, M. Positive and negative allosteric modulators of the Ca2+-sensing receptor interact within overlapping but not identical binding sites in the transmembrane domain. *J. Biol. Chem.* **2004**, *279*, 18990–18997.

(91) Petrel, C.; Kessler, A.; Maslah, F.; Dauban, P.; Dodd, R. H.; Rognan, D.; Ruat, M. Modeling and mutagenesis of the binding site of Calhex 231, a novel negative allosteric modulator of the extracellular Ca2+-sensing receptor. *J. Biol. Chem.* **2003**, *278*, 49487–49494.

(92) Miedlich, S. U.; Gama, L.; Seuwen, K.; Wolf, R. M.; Breitwieser, G. E. Homology modeling of the transmembrane domain of the human calcium sensing receptor and localization of an allosteric binding site. *J. Biol. Chem.* **2004**, *279*, 7254–7263.

(93) Jiang, P. H.; Cui, M.; Zhao, B. H.; Liu, Z.; Snyder, L. A.; Benard, L. M. J.; Osman, R.; Margolskee, R. F.; Max, M. Lactisole interacts with the transmembrane domains of human T1R3 to inhibit sweet taste. *J. Biol. Chem.* **2005**, *280*, 15238–15246.

(94) Jiang, P. H.; Cui, M.; Zhao, B. H.; Snyder, L. A.; Benard, L. M. J.; Osman, R.; Max, M.; Margolskee, R. F. Identification of the cyclamate interaction site within the transmembrane domain of the human sweet taste receptor subunit T1R3. *J. Biol. Chem.* **2005**, *280*, 34296–34305.

(95) Verdonk, M. L.; Berdini, V.; Hartshorn, M. J.; Mooij, W. T. M.; Murray, C. W.; Taylor, R. D.; Watson, P. Virtual screening using protein-ligand docking: Avoiding artificial enrichment. *J. Chem. Inf. Comput. Sci.* **2004**, *44*, 793–806.

(96) Ferrara, P.; Gohlke, H.; Price, D. J.; Klebe, G.; Brooks, C. L. Assessing scoring functions for protein-ligand interactions. *J. Med. Chem.* **2004**, *47*, 3032–3047.

(97) Perola, E.; Walters, W. P.; Charifson, P. S. A detailed comparison of current docking and scoring methods on systems of pharmaceutical relevance. *Proteins* **2004**, *56*, 235–249.

(98) Cole, J. C.; Murray, C. W.; Nissink, J. W. M.; Taylor, R. D.; Taylor, R. Comparing protein-ligand docking programs is difficult. *Proteins* **2005**, *60*, 325–332.

(99) Xing, L.; Hodgkin, E.; Liu, Q.; Sedlock, D. Evaluation and application of multiple scoring functions for a virtual screening experiment. *J. Comput.-Aided Mol. Des.* **2004**, *18*, 333–344.

(100) Muegge, I.; Martin, Y. C.; Hajduk, P. J.; Fesik, S. W. Evaluation of PMF scoring in docking weak ligands to the FK506 binding protein. *J. Med. Chem.* **1999**, *42*, 2498–2503.

(101) Unity Chemcial Information Software, Tripos Inc., St. Louis, MO.

(102) Daylight Chemical Information Software, Daylight Chemical Information Systems, Inc., Mission Viejo, CA.

(103) MACCS II, Molecular Design Ltd., San Leandro, CA.

CI8000265